Marine Chemistry 180 (2016) 51–56

Contents lists available at ScienceDirect

Marine Chemistry

journal homepage: www.elsevier.com/locate/marchem

Molecular diffusion of CF_3SF_5 in pure water and artificial seawater

Jonathan Vardner [a,*], Brice Loose [b]

[a] Worcester Polytechnic Institute, 100 Institute Rd, Worcester, MA 01609, USA
[b] Graduate School of Oceanography, University of Rhode Island, 215 South Ferry Rd, Narragansett, RI 02882, USA

ARTICLE INFO

Article history:
Received 10 June 2015
Received in revised form 23 January 2016
Accepted 25 January 2016
Available online 28 January 2016

Keywords:
Tracers
Diffusion coefficients
Gas chromatography
Mixing ratio

ABSTRACT

We have experimentally determined the diffusion coefficient for trifluoromethyl sulfur pentafluoride (CF_3SF_5) in pure water and artificial seawater over a temperature range of −2.0 °C to 30.0 °C. A working gas standard containing known concentrations of CF_3SF_5 and sulfur hexafluoride (SF_6) was prepared. The working standard was allowed to diffuse across a water barrier, stabilized with agar gel, and the diffused gas was swept into a gas chromatograph with an electron-capture detector to measure the resulting gas mixing ratio. The mixing ratios for both CF_3SF_5 and SF_6 were measured to determine the diffusivity for each species. The diffusion coefficient for SF_6 was determined during these experiments as a check against existing literature values and to validate our experimental setup. The experimental data were fit to the Arrhenius equation to yield the following equations $D_{CF_3SF_5} = 0.0015\exp(-12.9/RT)$ and $D_{SF_6} = 0.037\exp(-19.8/RT)$, where R is the gas constant in units of kilojoules per mole per kelvin and T is the temperature in kelvin. At the mean temperature of the ocean, 18 °C, $D_{CF_3SF_5} = 7.02\times10^{-6} \pm 9.9\%$ and $D_{SF6} = 1.03\times10^{-5} \pm 13.8\%\,cm^2/s$. The diffusion coefficients for SF_6 matched the literature data within 4.3% for all temperatures.

1. Introduction

Trifluoromethyl sulfur pentafluoride (CF_3SF_5) is an inert halocarbon in the class of gases collectively referred to as ignoble gases for the non-reactive properties they share with the noble gases, but also for their potentially deleterious environmental impacts. For example, the chlorofluorocarbons, also ignoble gases, are responsible for stratospheric ozone depletion (Solomon, 1999). CF_3SF_5 is similar in many respects to sulfur hexafluoride (SF_6), a gas used extensively in industry to electrically insulate high voltage equipment. Both CF_3SF_5 and SF_6 absorb radiation strongly in the infrared spectrum, making them greenhouse gases: CF_3SF_5 and SF_6 have 18,000 and 23,900 times the global warming potential (GWP) of CO_2, respectively (Sturges et al., 2000). CF_3SF_5 has no known industrial use and its anthropogenic source remains unknown. Its existence was previously thought to be the result of electrolytic degradation of SF_6; however Pepi et al. (2005) determined that this is not the case. Globally, both gases exist at the part per trillion level in the atmosphere and their concentrations are increasing at a rate of about 6% per year (Suen, 2008).

The electronegativity (or insulating property) of these two gases makes them detectable at extremely low concentrations by using gas chromatography with electron capture detection. This, in combination with the fact that they are inert and nearly non-existent in the natural environment, makes them potentially useful tracers for physical processes. SF_6 has been used extensively in tracer release experiments (TREs), providing a better understanding to many aspects of oceanography and environmental fluid mechanics (e.g., Ho et al., 2002; Ledwell et al., 2000). Recently, Law and Watson (2001); Tanhua et al. (2004), and Bullister et al. (2006) have determined that SF_6 can be potentially used as a transient tracer in the ocean, given its rate of monotonic increase in the atmosphere (Geller et al., 1997; Maiss and Brenninkmeijer, 1998). There is currently a high demand for a new transient tracer because the previously used chlorofluorocarbons have lost their effectiveness as a result of their declining atmospheric mixing ratios. It can become problematic if SF_6 is used in both TREs and as a transient tracer, because purposefully introduced SF_6 violates the boundary conditions provided by its well known atmospheric time history. Therefore, CF_3SF_5 has been adopted as a new tracer for TREs, so that SF_6 can become a dedicated transient tracer (Ho et al., 2008). Because of its potential value as a transient tracer, the scientific community has declared a moratorium on deep ocean tracer releases of SF_6 to avoid further contaminating the anthropogenic signal in the ocean.

Ho et al. (2008) determined that CF_3SF_5 has the potential to replace SF_6 in deep ocean TREs. CF_3SF_5 has several properties that make it a potential tracer. As stated above, it shares many of the ideal tracer properties with SF_6, and current experimental methods can be readily adapted to include measurement of both CF_3SF_5 and SF_6, which utilize the same techniques for injection, sampling, and analysis. Recently, the use of CF_3SF_5 has become more common; for instance the species was released in Drake Passage to determine ocean mixing at mid-depths (Watson et al., 2013). When interpreting the results of TREs with CF_3SF_5, it is valuable to determine the physical properties of the tracer, including its diffusivity in water. In dual-tracer gas exchange

* Corresponding author.
E-mail addresses: jtvardner@gmail.com (J. Vardner), brice@gso.uri.edu (B. Loose).

http://dx.doi.org/10.1016/j.marchem.2016.01.005
0304-4203/

experiments, for instance, two tracers with different diffusivities are released simultaneously, and the change in concentration ratio between the two species over time can determine gas exchange rates (Watson and Ledwell, 2000). In this experiment we determine the diffusivity of CF_3SF_5 in pure water as well as artificial seawater over a temperature range of −2 °C to 30 °C.

2. Experimental method

We have reproduced the experimental configuration used by King and Saltzman (1995), including use of the same diffusion cells, which were provided by Eric Saltzman. The experimental method was based on the ideas developed by Barrer (1941). A gas standard of known composition is allowed to diffuse across a water barrier while the concentration of the diffused gas is monitored on the other side of the cell. At steady state, the flux across the water barrier takes the form of Fick's First Law:

$$\Phi = \frac{D\Delta C}{l} \tag{1}$$

where Φ is the flux, D is the diffusion coefficient, ΔC is the difference in concentration across the water barrier, and l is the height of the water barrier (King and Saltzman, 1995). Since the solubility of CF_3SF_5 in water has been determined by Busenberg and Plummer (2008), the flux can be rewritten in terms of the gas solubility on each side of the water barrier. The diffusion coefficient for CF_3SF_5 in water can then be expressed as:

$$D = \frac{X_2 f_2 l}{X_1 \alpha A} \tag{2}$$

where X_1 is the gas mixing ratio before diffusing through the water barrier, X_2 is the gas mixing ratio after diffusing through the water barrier, f_2 is the volumetric flow rate of the diffused gas, α is the Ostwald solubility, and A is the cross-sectional area of the water barrier (Fig. 1).

The primary experimental challenge with measuring the aqueous diffusivity of gas arises from the large difference in gas concentration between X_2 and X_1. For sparingly soluble gases, such as these, X_2 can be five orders of magnitude smaller than X_1. A working gas standard containing CF_3SF_5 and SF_6 was prepared by serial dilutions using pressurized N_2 gas as the primary diluent. The targeted mixing ratios for CF_3SF_5 and SF_6 were 119 ppmv and 476 ppmv, respectively. These mixing ratios were chosen to produce a value for X_2 that would be in the calibration range of our third party gas standards. SF_6 was included in the working standard, as its diffusion coefficient could be determined to validate the experiment; the diffusion coefficient for SF_6 was determined and compared to the values obtained by King and Saltzman (1995).

To measure the exact concentration in our working gas standard (X_1) it was necessary to serially dilute the standard before injecting it directly into the gas chromatograph. Two Kimax® 1000 ml flasks were weighed, filled with DI water at room temperature, and then reweighed to accurately determine their volumes. The flasks were then purged with nitrogen at 5 psi for 5 min before being covered at atmospheric pressure with septum stoppers. A Hamilton MICROLITER™ syringe was used to inject the flasks with known volumes between 150 and 300 μl of the standard gas, making the pressure within the flasks marginally above atmospheric. We assumed that the septum stoppers absorbed or released very little amounts of gas. The potential contamination of the standard by adsorption and release of gas was not particularly significant because the concentration of the gas was approximately the same within the flask between trials. We equipped a 50 ml syringe with a needle to penetrate the septum stoppers and obtain the gas. The diluted gas solution was then injected into a VICI® 8-port valve where it loaded a 25 μl sample loop. Ultra high purity nitrogen purged the gas in the sample loop into a SRI 8610C gas chromatograph (GC) with an electron capture detector (ECD). The concentration of the diluted gas was determined by linearly interpolating between data points on a calibration curve for CF_3SF_5 (Fig. 2) and another calibration curve for SF_6 (Fig. 3). The calibration curves were prepared by injecting a 7.7 ppbv CF_3SF_5 standard and a 155.9 ppbv SF_6 standard into 10 μl, 25 μl, 100 μl, 0.25 ml, and 1.0 ml, sample loops. Three trials were conducted for each sample loop size, and the ECD consistently produced peak areas within a 0.5% relative error. To account for the drift in the ECD readings over time, the peak areas for each concentration measurement were bracketed by two points on the calibration curves within a few days. The use of a local piecewise linear fit rather than a polynomial fit was deemed satisfactory due to the proximity of each calibration point on the curve; therefore complete calibration curves utilizing the entire range of sample loop sizes were not prepared regularly. The dilution step of the standard gas was designed to locate the peak areas of the diluted gas in regions of the calibration curves where concentrations of each gas component could be accurately measured.

The gas mixing ratio at the outlet of the diffusion cell (X_2) was determined using the experimental method illustrated in Fig. 1. The standard gas flowed from its gas cylinder, through 1/8 inch inner diameter stainless steel tubing and into a flow controller (Cole Parmer 32907-67) to meter the gas at 0.003 standard liters per minute. The flow of gas then

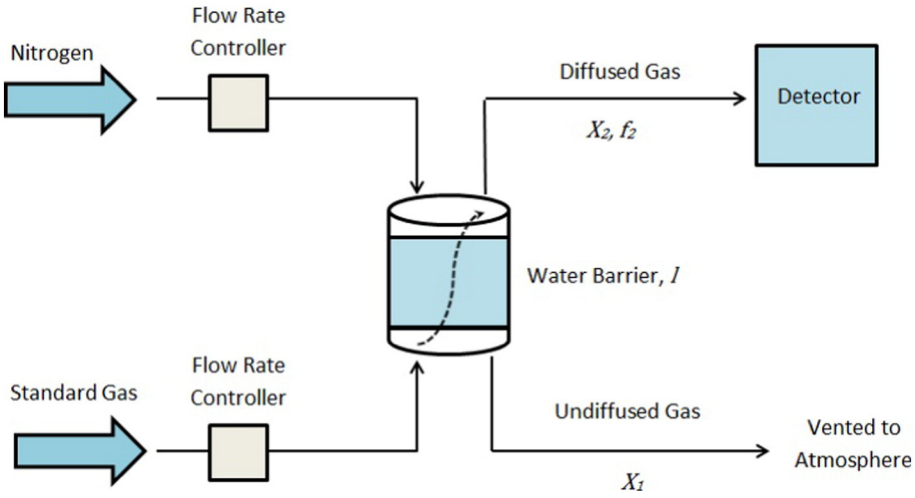

Fig. 1. A schematic of the experimental method used to diffuse the standard gas across a water barrier. The CF_3SF_5 and SF_6 concentrations were monitored using gas chromatography with an electron capture detector. The concentrations were monitored until the process reached steady state.

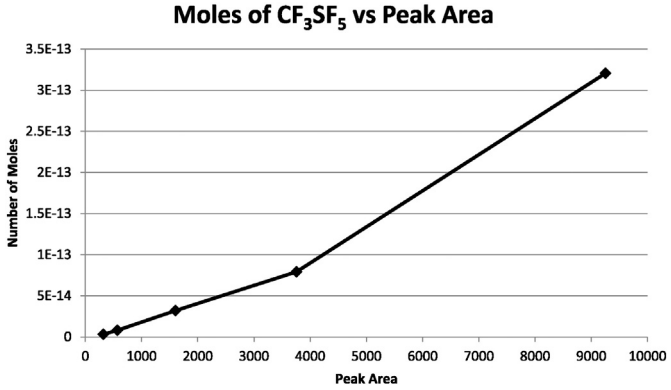

Fig. 2. An example of a calibration curve used for CF_3SF_5. The peak areas from diffusivity experiments were bracketed with known standards. A piece-wise linear fit was used to measure concentration. The majority of concentration measurements resulted in peak areas in the range of 5000–8000. The relative error for each point on the calibration curve was under 0.62%.

passed through 1/8 inch inner diameter vinyl tubing and into a diffusion cell housing the water barrier. The diffusion cell consists of a lower chamber below the water barrier and an upper chamber above the water barrier. The water barrier is supported by a porous hydrophobic filter membrane and a thin sheet of porous polyethylene (King and Saltzman, 1995). The rate of diffusion through the polyethylene sheet was assumed to be much greater than the rate of diffusion through the water barrier, and therefore the effects of the polyethylene sheet were negligible. The undiffused gas passed through the lower chamber and was vented to the atmosphere. The standard gas diffused from the lower chamber, through the water barrier, and into the upper chamber of the diffusion cell. A continuous flow of Ultra High Purity nitrogen then swept the diffused gas from the upper chamber into a VICI 8-port valve equipped with a sample loop. Before a sample was analyzed, a solenoid valve closed for 30 s to let the total pressure in the VICI valve equilibrate to atmospheric pressure. Finally, the VICI valve was rotated to introduce the sample onto the GC column for analysis. The concentration of the diffused gas was determined by linearly interpolating data points on the calibration curves. The operating conditions were designed to position the peak areas of CF_3SF_5 and SF_6 in the same region on the calibration curves as the X_1 measurements. The peak areas in the diffusivity experiments were bracketed by points on the calibration curves every few days to account for any drift in the ECD readings. Two trials for CF_3SF_5 concentration measurements (one trial at −2 °C and another trial at 15 °C) were slightly outside the range of calibration; however they were very close to a measured peak area and therefore their

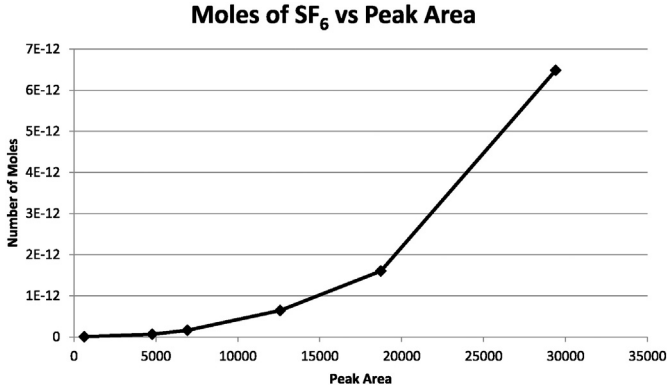

Fig. 3. An example of a calibration curve used for SF_6. A piece-wise linear fit was used to measure concentration. The flow rate of nitrogen was adjusted to position the diffused gas concentration in the most linear region of the calibration curve (a peak area of 7000–12,000). The dilution step positioned the diluted gas in the same region of the curve. The relative error for each point on the calibration curve was under 0.45%.

concentration measurements were deemed accurate. The accuracy of these trials was verified by the fact that the resulting diffusivity measurements agreed with the measurements of other trials. The uncertainty in concentration measurements of CF_3SF_5 and SF_6 were approximated to be 12.4% and 13.8%, respectively by applying the method of least squares to the ranges that were used in the calibration curves. The error in the concentration ratio (X_2/X_1) was reduced, however, since the measurements for X_2 and X_1 fell within the same region of the curves. The concentration values were likely overestimated considering that a polynomial fit would result in concentrations less than a piece-wise linear fit of the same data set. This overestimation, however, was divided out to some extent when X_2 was divided by X_1. Therefore, the error in the concentration ratios was less than the error in the concentration measurements, though the error in the concentration ratios cannot be quantified analytically. The concentration of the diffused gas was measured every 14 min to monitor when the diffusion process reached steady state. The process took 4–14 h to reach steady state depending on the temperature and thickness of the water barrier in the diffusion cell.

The water barrier consisted of an agar solution approximately 0.8% by mass. A gas permeable Millipore 10 μm membrane filter was used to support the agar solution in the diffusion cell. The height of the water barrier (l) was determined by measuring the mass of the agar solution placed into the diffusion cell. We varied the water barrier height between trials to prevent the standard gas from penetrating through the space in between the water barrier and diffusion cell. The variability in height was accounted for using the proportionality between water barrier thickness and diffusivity. The mass of the agar solution after the diffusion process was used to calculate the gel thickness. Thomas and Langdon (1971) determined that the use of agar solution rather than pure water decreased the calculated diffusion coefficients by approximately 1.9%. Therefore, all the diffusion coefficients were increased by 1.9% to account for the effect of the agar solution. The flow rate of the diffused gas (f_2) was metered at the inlet to the top of the diffusion chamber using a (Cole Parmer 32907-67) flow controller. Depending on the temperature of each trial, we set the nitrogen flow rate between values of 0.004 and 0.020 l per minute. Higher flow rates generally corresponded to lower temperatures. The flow of gas across the water barrier was held constant during an experiment. We adjusted the flow rate, f_2, of nitrogen to control the moles of gas that collected in the sample loop. We chose appropriate flow rates of nitrogen for each trial to position the measured ECD readings within the calibrated range. The Ostwald solubilities for SF_6 and CF_3SF_5 were determined using relationships developed by Bullister et al. (2002) and Busenberg and Plummer (2008). The solubility determinations for SF_6 in pure water and seawater occurred over a temperature range of 0 °C to 40 °C. Here, we have applied the solubility relationships for SF_6 slightly outside the range of determination, when measuring diffusivity at −2 °C. The Ostwald solubility of CF_3SF_5 in pure water (α) was measured over a temperature range of 1 °C to 35 °C, and again, we applied our solubility relationship slightly outside the range of determination when measuring diffusivity at −2 °C. The Ostwald solubility of CF_3SF_5 in seawater, however, was not measured and therefore an approximate value was determined. We found the solubility ratio of CF_3SF_5 to SF_6 in pure water and assumed that the same solubility ratio applied for seawater. The solubility ratio, CF_3SF_5:SF_6, was 0.53,0.54, 0.53, and 0.48 at temperatures of −2 °C, 3 °C, 15 °C, and 30 °C, respectively. Solubility decreased with temperature for all temperature ranges except for −2 °C to 3 °C; this indicates uncertainty in extrapolating measurements for solubility beyond the measured data set. The adjustment of the nitrogen flow increased the pressure within the upper chamber of the diffusion cell by at most 0.37 kPa above atmospheric pressure for some trials in this study. The small increase in pressure was measured using the (Cole-Parmer 32907-67) flow controller located on the tubing leading up to the upper chamber of the diffusion cell. The flow of the standard gas increased the pressure within the lower chamber of the diffusion cell by

at most 0.04 kPa above atmospheric pressure and was measured using the (Cole-Parmer 32907-67) flow controller leading up to the lower chamber of the diffusion cell. We assumed that the total pressures measured by the two flow controllers were equal to the total pressure in the upper and lower chambers of the diffusion cell. We adjusted the resulting estimate of the Ostwald solubility to account for this increase in pressure in the lower chamber of the cell. The surface area of the water barrier (A) was determined by measuring the diameter of the diffusion cell.

Stable temperature was maintained using a constant temperature bath filled with saltwater to an approximate salinity of 40 ppt, to allow the bath water to be cooled to −2.0 °C. The temperature of the diffusion cell was closely monitored using an Omega 1PT100K3515 100 Ohm 4-wire RTD taped to the outside of the cell. The high thermal mass of the stainless steel diffusion cell added an additional measure of thermal stability. Diffusion experiments were conducted at −2.0 °C, 3.0 °C, 15.0 °C and 30.0 °C in DI water, and again at the same temperatures using a 35 ppt solution of Instant Ocean® artificial seawater to find the diffusion coefficient in seawater over the same range in temperature. Salinity was measured with a YSI Pro Plus multiparameter meter with conductivity sensor. Two trials in DI water and two trials in artificial seawater were completed at each temperature, for a total of N = 4 separate determinations of the diffusion coefficient of CF_3SF_5 and SF_6 at each temperature, except at −2 °C where two trials were completed in DI water and one trial was completed in artificial seawater.

Considering the uncertainty in the concentration ratio (stated above) as well as the uncertainties in the gel thickness and solubility, we estimate the uncertainty of a diffusivity experiment to be at most 18–19% for the diffusivity measurements of SF_6 and CF_3SF_5. These uncertainties were determined using the error in concentration of the gases rather than the error in concentration ratio of the gases. Since the error in concentration ratio was less than the error in gas concentration, as stated above, the uncertainties are likely overestimated. Although the concentration measurement was more accurate for CF_3SF_5 than SF_6, the solubility was less accurate because the solubility in seawater was not directly measured. As a result, the estimated uncertainties were approximately equal for each species.

3. Results and discussion

The concentrations of CF_3SF_5 and SF_6 in the working standard were found to be 1716 and 776 ppmv respectively. The reason that the CF_3SF_5 concentration greatly exceeded the target concentration is not known, but may be the result of an incomplete step in the gas standard preparation, which was carried out without direct analytical control of the gas mixing ratio. The dilution step involved in determining the standard gas concentration introduced an uncertainty of 2.9% for CF_3SF_5 and 3.5% for SF_6 in the diffusivity values.

The thickness of the water barrier varied from 0.33–0.57 cm with an average value of 0.45 ± 0.073 cm between trials. The surface area of the diffusion cell was determined to be 11.7 cm^2.

3.1. Diffusion in DI water and seawater

The measured diffusivity for each species in seawater was similar to the measured diffusivities in DI water (Figs. 4 and 5). The observed differences between the seawater and DI water trials were not systematic, and it was not possible to separate the variability introduced from experimental error. This result for SF_6 agreed with the work of King and Saltzman (1995) where there was also no consistent difference in the SF_6 diffusion coefficient between pure and salt water. It is generally expected for diffusivity to be lower in seawater than in pure water due to seawater's increased ionic strength and viscosity. This demonstrates the lack of knowledge about the diffusion process. There is no current theory that can accurately predict the effect of ionic strength on the diffusion of a gas through a liquid barrier. Consequently, we report the diffusivity values and statistics after aggregating the saltwater and DI water trials.

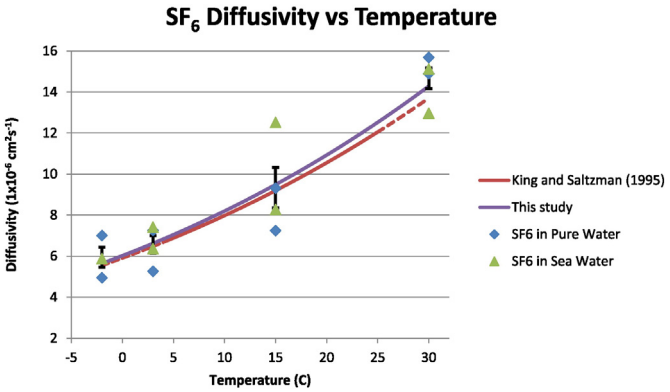

Fig. 4. Diffusion coefficients for SF_6 in pure water and sea water compared to the equation of King and Saltzman (1995). The results for the pure water and seawater measurements were aggregated in the Arrhenius model. The error bars present the standard error for diffusivity at each measured temperature. The results for this experiment were in agreement with previous studies, particularly at lower temperatures. The dashed portions of the line from the King and Saltzman (1995) equation depict where the equation is extrapolated beyond the measured range. The equation for this study is: $D_{SF_6} = 0.037 \exp(-19.8/RT)$.

3.2. Diffusion of SF_6 in water

The diffusion coefficient can be related to temperature with the Arrhenius equation, as shown below:

$$D = A \exp\left(-\frac{Ea}{RT}\right) \quad (3)$$

where Ea is the activation energy in kilojoules per mole, R is the gas constant in kilojoules per mole per kelvin, T is the temperature in kelvin, and A is the preexponential factor in square centimeters per second. The values for the activation energy and preexponential factor are determined using the best linear fit to the natural log of diffusivity (dependent variable) and the reciprocal of temperature (independent variable). The activation energy was found to be 19.8 kJ $mole^{-1}$ and the preexponential factor was found to be 0.037 cm^2 s^{-1} for the diffusivity of SF_6 in water. The overall uncertainty of this fit was 1σ = 13.8%, as determined by applying the method of least squares to the Arrhenius model. The measured data points and equation are shown alongside the equation from King and Saltzman (1995) in Fig. 4.

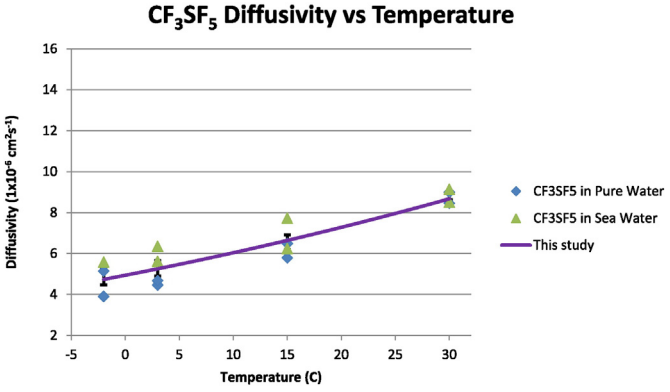

Fig. 5. Diffusion coefficients of CF_3SF_5 in pure water and sea water. The results for the pure water and seawater measurements were aggregated in the Arrhenius model. The error bars present the standard error for diffusivity at each measured temperature. The CF_3SF_5 diffusion coefficients were lower than the SF_6 diffusion coefficients, as expected due to its increased molecular mass. The equation for this study is: $D_{CF_3SF_5} = 0.0015 \exp(-12.9/RT)$.

The measured SF_6 diffusion coefficients were slightly larger than the values measured by King and Saltzman (1995). The diffusivity given from our equation was approximately 1.8%, 2.2%, 3.1%, and 4.3% larger than the diffusivity from these authors' equation at temperatures of −2.0 °C, 3.0 °C, 15.0 °C, and 30.0 °C, respectively. The discrepancy between our data and the data of King and Saltzman (1995) is within our experimental uncertainty and therefore deemed to be an acceptable agreement. King and Saltzman (1995) determined diffusivity of SF_6 over a temperature range of 5.0 °C to 25.0 °C, which we extrapolated to a range of −2.0 °C to 30.0 °C.

In this experiment the standard error between trials of the same temperature at −2.0 °C, 3.0 °C, 15.0 °C, and 30.0 °C were 8.2%, 6.5%, 10.6%, and 3.5%, respectively. The uncertainty can be attributed to several factors. Primarily, there was an error in the determination of concentrations from the calibration curves. Furthermore, the hydrophobic Millipore membrane filters repelled the agar solution in the diffusion cell, creating a slightly variable agar gel thickness. In addition, there was some error in integrating the peak areas produced by the ECD; for instance some water in the agar gel evaporated at higher temperatures, which produced broad peaks that altered the baseline for peaks produced by SF_6. Lastly, there was error in the solubility values due to the pressure gradient across the diffusion cell as well as the extrapolation of solubility values to a temperature range that was not directly measured. The solubility of SF_6 decreased with increasing temperature, and consequently, lower temperatures resulted in more transport of SF_6 into the ECD than higher temperatures. We aimed to control the transport of gas into the ECD by adjusting the N_2 flow rate (f_2); however, some trials at lower temperature resulted in greater peak areas on the calibration curves than higher temperatures. The calibration of large peak areas was less accurate than the calibration of small peak areas because the calibration curves developed curvature as peak area increased. Consequently, measured diffusivities tended to have lower values for standard deviation at higher temperatures than lower temperatures.

3.3. Diffusion of CF_3SF_5 in water

The activation energy and preexponential factor were found using the same method as SF_6 and were found to be 12.9 kJ mole^{-1} and 0.0015 cm^2 s^{-1}, respectively. The overall uncertainty was $1\sigma = 9.9\%$. The results are presented graphically in Fig. 5. The standard error between trials of the same temperature at −2.0 °C, 3.0 °C, 15.0 °C, and 30.0 °C were 8.5%, 7.2%, 5.4%, and 1.7%, respectively. The uncertainty can be attributed to the same variability in the analytical procedure as stated above.

The value of D for CF_3SF_5 was approximately 25% less than the value of D for SF_6 in the temperature range of −2.0 °C to 15.0 °C, and approximately 35% less than the D for SF_6 at 30.0 °C. Based on the Graham's Law relationship, which relates molecular kinetics to the square root of the reciprocal of molecular mass, it makes sense for CF_3SF_5 to have lower diffusivity than SF_6 in water due to its larger molecular mass. We applied Graham's Law to our measured diffusivities of SF_6 to determine theoretical diffusivities for CF_3SF_5. We then plotted the measured diffusivities for CF_3SF_5 against the theoretical values from Graham's Law, as shown in Fig. 6. Diffusivity for CF_3SF_5 was generally less than expected from Graham's Law, particularly at high temperatures. Graham's Law is known to approximately model the diffusion process, and therefore, the deviation from Graham's Law is reasonable. At temperatures of −2.0 °C, 3.0 °C, 15.0 °C, and 30.0 °C, the measured CF_3SF_5 diffusivity was 5.0%, 7.0%, 18.6%, and 30.7% less than the theoretical Graham's Law value, respectively. Therefore, the deviation from Graham's Law increases with temperature. Previous estimates for CF_3SF_5 diffusivity that were obtained by applying Graham's Law to the SF_6 diffusivity model from King and Saltzman (1995) are also overestimated; at the mean temperature of the ocean, 18 °C, the theoretical value for CF_3SF_5 diffusivity is 22.9% greater than our determined value. Consequently, studies

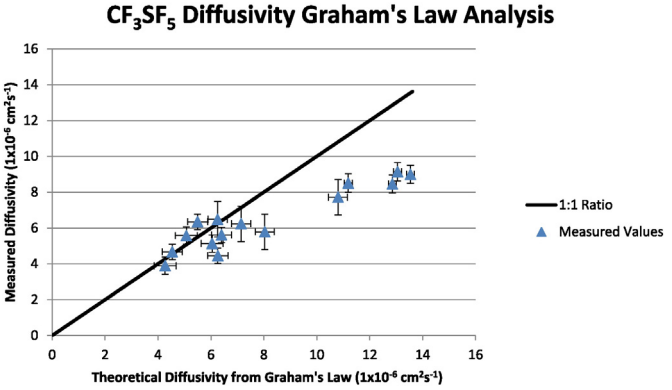

Fig. 6. Measured diffusion coefficients of CF_3SF_5 compared to theoretical results from Graham's Law. The 1:1 ratio line presents the points where measured diffusivity is equal to theoretical diffusivity from Graham's Law. The vertical error bars present the error in CF_3SF_5 diffusivity measurements. The horizontal error bars present the error in SF_6 diffusivity measurements, which were used directly in the Graham's Law analysis.

that estimated CF_3SF_5 diffusivity from Graham's Law relationships would benefit from a reevaluation of data using the diffusivity values measured in this experiment.

3.4. Impacts of measured diffusivities

Based upon our experimental setup and the estimated uncertainty in D_{SF_6} (13.8%), we do not conclude that the 5% increase in D_{SF_6} is significantly different from the previous results of King and Saltzman (1995). Here, we included SF_6 as a test of the reproducibility of the method and as a confirmation that our experimental configuration was consistent with previous experiments. Knowledge of the effective diffusivity of CF_3SF_5 is pertinent information for the potential candidate's use as a gas-exchange tracer, similar to the way SF_6 is currently used. The information is also important to estimate tracer loss if CF_3SF_5 is to be used in mixing experiments (e.g., Ho et al., 2002). Although the diffusivity of CF_3SF_5 is lower than expected, it still may not be practical to consider CF_3SF_5 and SF_6 as a practical tracer duet for open ocean dual tracer experiments. Currently ^{3}He and SF_6 are used for dual tracer experiments; however ^{3}He is difficult to measure, so an alternative pairing is desirable. Nevertheless, the evolution of the concentration ratio of SF_6 and CF_3SF_5 is less than 20% in 30 days, as compared with a change of 94% in the concentration ratio of ^{3}He and SF_6 (Fig. 7).

4. Conclusion

The diffusivity for SF_6 and CF_3SF_5 in pure water and artificial seawater was measured over a temperature range of −2 °C to 30 °C. The diffusivity of each species did not differ considerably between pure water and seawater; therefore the Arrhenius equation models were used to fit diffusivity in pure water and seawater equally well. This result agreed with previous studies, where the diffusion coefficient for SF_6 did not consistently differ between pure water and seawater. The measured diffusivity of SF_6 in water followed the expression: $D_{SF_6} = 0.037\exp(-19.8/RT)$ with an overall uncertainty of 13.8% in the fit of the model to the data. Similarly, the measured diffusivity of CF_3SF_5 in water followed the expression: $D_{CF_3SF_5} = 0.0015\exp(-12.9/RT)$ with an overall uncertainty of 9.9% in the fit of the model to the data. The measured diffusion coefficient for SF_6 in water was in reasonable agreement with previous studies, validating the method used to measure the diffusion coefficient for CF_3SF_5. Previous estimates for CF_3SF_5 diffusivity from Graham's Law relationships overestimate diffusivity, and therefore a reevaluation of data using measured values for diffusivity would be beneficial. Although the measured diffusivity for CF_3SF_5 is lower than expected, it is not practical to use CF_3SF_5 and SF_6 together in dual tracer experiments

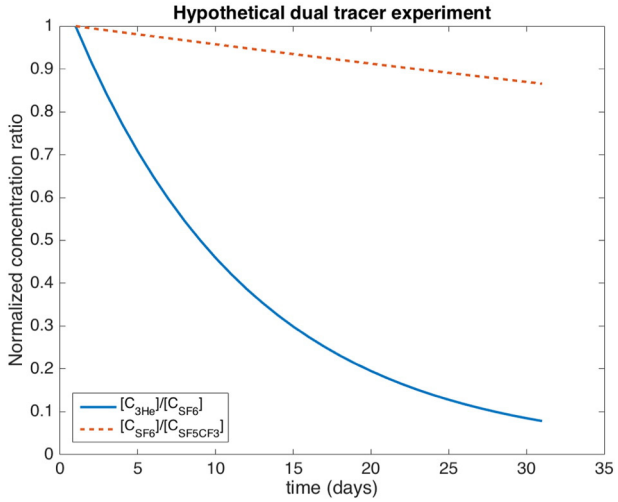

Fig. 7. Normalized concentration ratio of ^{3}He:SF_6 and SF_6:SF_5CF_3 within a hypothetical dual tracer experiment. Parameters used were a gas transfer velocity of $k_{660} = 5$ m d^{-1}, mixed-layer depth of 50 m, water temperature of 0 °C, and salinity of 34 g/kg. At 0 °C, we used diffusivity values of 4.94×10^{-6}, 6.05×10^{-6}, and 4.3×10^{-5} cm^2 s^{-1} for CF_3SF_5, SF_6, and ^{3}He, respectively.

because their values for diffusivity do not promote a rapid evolution in concentration ratio. The use of CF_3SF_5 in TREs will become more common as SF_6 becomes a dedicated transient tracer, and therefore, the measured diffusivity of CF_3SF_5 in water is significant; the measurements in this experiment provide researchers improved accuracy in the data analysis of TREs.

Acknowledgments

Thank you to Kathleen Donahue, David Smith, and Kim Carey for organizing the 2014 SURFO program. We would like thank Dennis Graham for the helpful discussion throughout the project and for providing the use of equipment. We would also like to thank Ann Lovely and Arash Bigdeli for their advice and support. Lastly, thank you to the National Science Foundation REU program for supporting the URI Summer Undergraduate Research Fellowship Opportunity (SURFO) program.

References

Barrer, R.M., 1941. Diffusion in and through solids. CUP Archive.
Bullister, J.L., Wisegarver, D.P., Menzia, F.A., 2002. The solubility of sulfur hexafluoride in water and seawater. Deep-Sea Res. I Oceanogr. Res. Pap. 49 (1), 175–187. http://dx.doi.org/10.1016/S0967-0637(01)00051-6.
Bullister, J.L., Wisegarver, D.P., Sonnerup, R.E., 2006. Sulfur hexafluoride as a transient tracer in the North Pacific Ocean. Geophys. Res. Lett. 33 (18), L18603. http://dx.doi.org/10.1029/2006GL026514.
Busenberg, E., Plummer, L.N., 2008. Dating groundwater with trifluoromethyl sulfurpentafluoride (SF_5CF_3), sulfur hexafluoride (SF_6), CF_3Cl (CFC-13), and CF_2Cl_2 (CFC-12). Water Resour. Res. 44 (2), W02431. http://dx.doi.org/10.1029/2007WR006150.
Geller, L.S., Elkins, J.W., Lobert, J.M., Clarke, A.D., Hurst, D.F., Butler, J.H., Myers, R.C., 1997. Tropospheric SF_6: observed latitudinal distribution and trends, derived emissions and interhemispheric exchange time. Geophys. Res. Lett. 24 (6), 675–678. http://dx.doi.org/10.1029/97GL00523.
Ho, D.T., Schlosser, P., Caplow, T., 2002. Determination of longitudinal dispersion coefficient and net advection in the tidal Hudson River with a large-scale, high resolution SF6 tracer release experiment. Environ. Sci. Technol. 36 (15), 3234–3241. http://dx.doi.org/10.1021/es015814+.
Ho, D.T., Ledwell, J.R., Smethie, W.M., 2008. Use of SF_5CF_3 for ocean tracer release experiments. Geophys. Res. Lett. 35 (4), L04602. http://dx.doi.org/10.1029/2007GL032799.
King, D.B., Saltzman, E.S., 1995. Measurement of the diffusion coefficient of sulfur hexafluoride in water. J. Geophys. Res. Oceans 100 (C4), 7083–7088. http://dx.doi.org/10.1029/94JC03313.
Law, C.S., Watson, A.J., 2001. Determination of Persian Gulf Water transport and oxygen utilisation rates using SF_6 as a novel transient tracer. Geophys. Res. Lett. 28 (5), 815–818. http://dx.doi.org/10.1029/1999GL011317.
Ledwell, J.R., Montgomery, E.T., Polzin, K.L., Laurent, L.C. St, Schmitt, R.W., Toole, J.M., 2000. Evidence for enhanced mixing over rough topography in the abyssal ocean. Nature 403 (6766), 179–182. http://dx.doi.org/10.1038/35003164.
Maiss, M., Brenninkmeijer, C.a.M., 1998. Atmospheric SF_6: trends, sources, and prospects. Environ. Sci. Technol. 32 (20), 3077–3086. http://dx.doi.org/10.1021/es9802807.
Pepi, F., Ricci, A., Di Stefano, M., Rosi, M., 2005. Gas phase protonation of trifluoromethyl sulfur pentafluoride. Phys. Chem. Chem. Phys. 7 (6), 1181–1186. http://dx.doi.org/10.1039/B416945J.
Solomon, S., 1999. Stratospheric ozone depletion: a review of concepts and history. Rev. Geophys. 37 (3), 275–316. http://dx.doi.org/10.1029/1999RG900008.
Sturges, W.T., Wallington, T.J., Hurley, M.D., Shine, K.P., Sihra, K., Engel, A., Oram, D.E., Penkett, S.A., Mulvaney, R., Brenninkmeijer, C.a.M., 2000. A potent greenhouse gas identified in the atmosphere: SF_5CF_3. Science 289 (5479), 611–613. http://dx.doi.org/10.1126/science.289.5479.611.
Suen, M., 2008. Trifluoromethyl sulfur pentafluoride (CF_3SF_5): a review of the recently discovered super-greenhouse gas in the atmosphere. Open Atmos. Sci. J. 2 (April), 56–60. http://dx.doi.org/10.2174/1874282300802010056.
Tanhua, T., Anders Olsson, K., Fogelqvist, E., 2004. A first study of SF_6 as a transient tracer in the Southern Ocean. Deep-Sea Res. II Top. Stud. Oceanogr. 51 (22–24), 2683–2699. http://dx.doi.org/10.1016/j.dsr2.2001.02.001 (The SWEDARP 1997/98 Expedition).
Thomas, H.C., Langdon, A.G., 1971. Self-diffusion studies of gel hydration and the obstruction effect. J. Phys. Chem. 75 (12), 1821–1826. http://dx.doi.org/10.1021/j100681a011.
Watson, A.J., Ledwell, J.R., 2000. Oceanographic tracer release experiments using sulphur hexafluoride. J. Geophys. Res. Oceans 105 (C6), 14325–14337. http://dx.doi.org/10.1029/1999JC900272.
Watson, A.J., Ledwell, J.R., Messias, M.-J., King, B.A., Mackay, N., Meredith, M.P., Mills, B., Naveira Garabato, A.C., 2013. Rapid cross-density ocean mixing at mid-depths in the drake passage measured by tracer release. Nature 501 (7467), 408–411. http://dx.doi.org/10.1038/nature12432.